

# A simple algorithm to place equal-mass SPH particles to realize discs with arbitrary radial density profiles

Satoko Yamamoto,<sup>1,2\*</sup> Natsuki Hosono,<sup>2</sup> Yoko Funato<sup>3</sup> and Junichiro Makino<sup>2,4</sup>

<sup>1</sup>*Department of Earth & Planetary Sciences, Tokyo Institute of Technology, Ookayama, Meguro-ku, Tokyo 152-8550, Japan*

<sup>2</sup>*RIKEN Advanced Institute for Computational Science, Minatojima-minamimachi, Chuo-ku, Kobe, Hyogo 650-0047, Japan*

<sup>3</sup>*General Systems Studies, University of Tokyo, Komaba, Meguro-ku, Tokyo 153, Japan*

<sup>4</sup>*Earth-Life Science Institute, Tokyo Institute of Technology, Ookayama, Meguro-ku, Tokyo 152-8550, Japan*

Accepted XXX. Received YYY; in original form ZZZ

## ABSTRACT

In this paper, we present a simple algorithm to realize discs of arbitrary radial density profiles by placing equal-mass particles on concentric rings. The realized disc shows very small density fluctuation, even after many rotations following differential rotation laws. Unlike the previously reported methods, our procedure is deterministic and does not require any manual adjustment.

**Key words:** hydrodynamics — methods: numerical.

## 1 INTRODUCTION

The capability of the SPH method to follow the evolution of thin and cold discs has been studied by a number of authors, and many new improvements of SPH methods have been proposed (Balsara 1995; Morris & Monaghan 1997; Imaeda & Inutsuka 2002; Cullen & Dehnen 2010; Hopkins 2015). If we look at results of very successful methods (e.g. Figure 6 of Hopkins 2015), however, we can see the disc shows large and apparently random density fluctuations.

These fluctuations have nothing to do with the problems in the treatment of hydrodynamics in SPH, since such fluctuations do appear in a purely keplarian disc. Figure 1 shows the particle distribution of purely keplarian disc, at time 0 and after 100 orbits (at the outer edge). Initially, particles are placed at Cartesian grid, and their positions at  $t = 200\pi$  are calculated using the angular velocity  $\omega = r^{-3/2}$ . We can see that the large density fluctuations have developed by  $t = 200\pi$ .

These large density fluctuations appear because the differential rotation of particles initially in the Cartesian grid effectively randomize their angular positions. As discussed in detail by Cartwright et al. (2009, hereafter C09), there are two obvious ways to prevent these fluctuations from growing.

One is to place particles at random. In this case, the fluctuations are initially there, and thus do not grow further in time. However, it is clear that this “solution” is far from ideal. We cannot express a disc with uniform density with any acceptable accuracy, even in the limit of the infinite number of particles, since the amplitude of the density

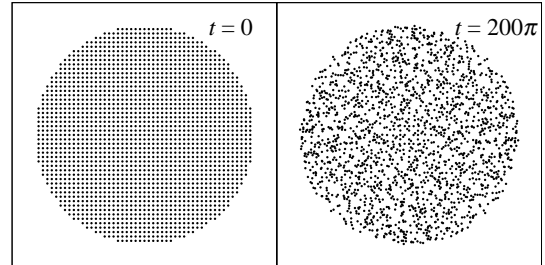


**Figure 1.** This figure shows the distribution of purely keplarian disc. The left-hand side shows the distribution at  $t = 0$  and the right-hand side shows that at  $t = 200\pi$ .

fluctuation is determined by the number of neighbour particles and not by the total number of particles. Moreover, the “density” of a particle changes in time, as the local neighbours change due to the differential rotation.

Another way is to place particles in concentric rings. This approach is certainly better than the first one, since the density fluctuation is initially very small and remains to be so, as far as particles move on purely circular orbits.

In order to place particles in concentric rings, C09 introduced a method based on a spiral. The radial positions of particles are chosen as equal-spacing points in the radial mass coordinate, and angular displacement between neighbouring particles is then determined so that angular and radial intervals are similar. They introduced this rather complex method so that any radial density distribution can be

\* E-mail: yamamoto.s.an@geo.titech.ac.jp

expressed. However, since the resulted distribution is based on a spiral, they need to modify this spiral into concentric rings. Unfortunately, they did not present the detail of this modification procedure. Thus, it is not clear how this modification can be done and how much errors are generated in the density profile.

In this paper, we present a simple algorithm to place particles in concentric rings. Our algorithm is much simpler than the spiral-based one of C09 for the cases of power-law density profiles, and reasonably simple for general cases.

In section 2, we present our new algorithm for discs of uniform density and power-law density profiles. In section 3, we generalize our new algorithm so that it can model arbitrary radial profiles. The algorithms presented in this paper are implemented in our program "DISKS"<sup>1</sup>. All particle placement data used in this paper can be generated using DISKS. In section 4, we discuss related works and summarize our paper.

## 2 NEW ALGORITHM FOR UNIFORM AND POWER-LAW DISCS

In section 2.1, we present our algorithm for uniform (constant density) disc. Then in sections 2.2 and 2.3, we discuss how power-law discs can be generated with our algorithm. In section 2.4, we introduce an optimization for power-law discs.

### 2.1 Uniform disc

If we want to express a uniform disc with concentric rings of particles of equal mass, what we need to do is conceptually very simple. We generate some number of concentric rings with constant radial displacement. On each ring, we place particles whose number is proportional to the length, and thus the radius, of that ring.

Note that it is not always possible to place the required number of particles, since that number might not be an integral number. In order to guarantee that we can place integral numbers of particles to all rings, we propose the following very simple procedure.

Consider the case that we want to place around  $n$  rings between radius  $r_{\text{in}}$  and  $r_{\text{out}}$  ( $r_{\text{out}} > r_{\text{in}}$ ). Here, we assume that particles in the outermost ring are actually placed at radius  $r_{\text{out}}$ , and not at somewhere like the middle point between  $r_{\text{out}}$  and the nearest ring of  $r_{\text{out}}$ ,  $r_{\text{out}} - (r_{\text{out}} - r_{\text{in}})/(2n)$ . If we divide the range  $(r_{\text{in}}, r_{\text{out}})$  to  $n$  rings, it is not guaranteed that we can place an integral number of particles on each ring. However, if we divide  $(0, r_{\text{out}})$  to  $n_{\text{int}}$  rings, where  $n_{\text{int}}$  is the nearest integral number to  $nr_{\text{out}}/(r_{\text{out}} - r_{\text{in}})$ , we can place integral number of particles on each ring.

If we number the ring from the innermost one, the  $i$ -th ring has the radius  $ir_{\text{out}}/n_{\text{int}}$  ( $0 < i \leq n_{\text{int}}$ ). Therefore, for any positive integral number  $p$ , if we place  $pi$  particles on ring  $i$ , we have achieved our goal of placing particles so that the uniform density is realized.

The remaining question is how to choose an appropriate value for  $p$ . The radial displacement of rings is  $r_{\text{out}}/n_{\text{int}}$ , while that in the circumferential direction is  $2\pi r_{\text{out}}/(n_{\text{int}}p)$ . Therefore,  $p = 6$  would make the radial and the circumference separations the closest to each other.

Figure 2 shows the examples of particle placements with  $p = 4, 6$  and  $8$ . We set radius of each disc to unity. We can see that the distribution with  $p = 6$  makes the radial and the circumference separations closest, and thus the disc looks most "natural".

### 2.2 Power-law disc

We consider a disc with a power-law density profile given by

$$\Sigma(r) = \Sigma_0 r^\alpha, \quad (1)$$

where  $\Sigma(r)$  is the surface density,  $r$  is the radius, and  $\Sigma_0$  is a constant. We assume that  $\Sigma_0$  is  $1/(2\pi)$ , because this assumption does not affect the discussion. Here, we consider the transformation from a uniform-density disc to a disc given by equation (1) (hereafter power-law disc) using the radial mass coordinate. The mass inside  $r = r_{\text{uni}}$  of a uniform disc is given by,

$$M(r) = \frac{r_{\text{uni}}^2}{2}, \quad (2)$$

For a power-law disc, the mass inside  $r = r_{\text{pow}}$  is given by

$$M(r) = \frac{r_{\text{pow}}^{\alpha+2}}{\alpha+2}. \quad (3)$$

By requiring  $M(r)$  of equations (2) and (3) equal, we have

$$r_{\text{pow}} = \left[ \frac{(\alpha+2)}{2} r_{\text{uni}}^2 \right]^{1/(\alpha+2)}. \quad (4)$$

Note that this transformation is valid only for  $\alpha > -2$ .

For the case of  $\alpha = -2$ , an obvious way to distribute equal mass particles is to place rings in logarithmically equal spacing and place a constant number of particles on each ring.

For the case of  $\alpha < -2$ , we can actually use the same transformation equation (4) as in the case of  $\alpha > -2$ , but now the power-law disc has an inner edge at the unit radius and it extends to the infinity.

The optimal choice of  $p$  for the power-law disc depends the power index  $\alpha$ . From equation (4), we have

$$\frac{d \log r_{\text{pow}}}{d \log r_{\text{uni}}} = \frac{2}{(\alpha+2)}. \quad (5)$$

From equation (5), the distance between two neighbouring rings, normalized by the radius, is changed by this factor of  $2/(\alpha+2)$ . The radial distance between two neighbouring rings, normalized by the radius, are changed by this factor. For a uniform-density disc, we had

$$p \sim 2\pi, \quad (6)$$

to make the radial and the circumference separations equal. Thus, for a power-law disc with power index  $\alpha$ , we have

$$p \sim \pi(2+\alpha). \quad (7)$$

For  $\alpha < -2$ , we should take the absolute value of  $p$  and place particles from outer edge to inner edge. If the right-hand side of equation (7) is not an integer, we should use the nearest integer.

<sup>1</sup> A public code is available at <https://github.com/yamasato/DISKs>

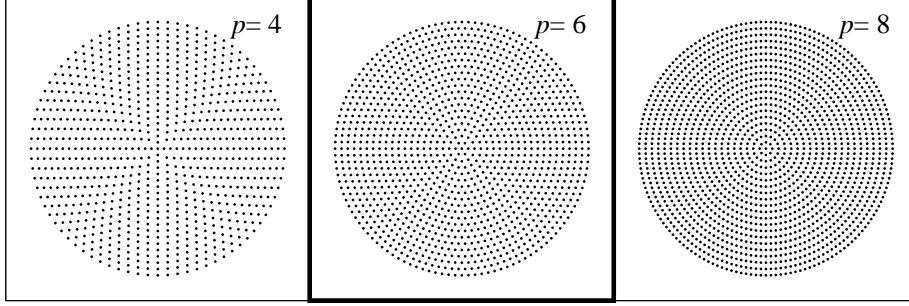


**Figure 2.** These are example of particle placements with  $p = 4, 6$  and  $8$ . The left-hand side shows the distribution with  $p = 4$  and the middle and the right-hand sides show that with  $p = 6, 8$ . The boxed disc with bold lines is plotted with the optimal choice of  $p$ .

Figure 3 show the examples of particle placements with  $p = 2, 3, 4, 5, 6$  for the density profiles with  $\alpha = -1.5, -1, -0.5, 0$ . Panels in thick boxes indicate optimal values of  $p$  for given  $\alpha$  as indicated in equation (7). We can see that they actually realized near-equal radial and circumferential separations of particles.

Note that particle placement generated this way has  $p$ -fold rotational symmetry. In particular for small  $p$ , this symmetry might cause a large systematic error in SPH force evaluation. One way to avoid this error is to randomly rotate each ring so that the correlation of particle locations between neighbouring rings is minimized. Figure 4 shows the result of such a random rotation. We can see that symmetric features clearly visible in figure 3 are erased.

### 2.3 The optimal placement for $p = 0$

With  $p = 0$ , the number of particles in a ring  $N$  is a free parameter. Therefore we derive the optimal  $m$  for the disc with  $p = 0$  as a function of  $N$  in this section.

First we consider the disc with  $\alpha = -2$ . Because the mass is a logarithmic function of radius,  $r_i$ , which is the radius at  $i$ -th ring, satisfies the following relation,

$$r_i = r_{i+1} e^{-mN/(2\pi\Sigma_0)}. \quad (8)$$

For the optimal value of  $m$ , the error  $\epsilon$  is minimized, where

$$\epsilon = \log \left| \frac{\delta r_{\text{cir}}}{\delta r_{\text{rad}}} \right|. \quad (9)$$

The parameter  $\delta r_{\text{cir}}$  is the average of circumference separations of ring  $i + 1$  and ring  $i$ ,

$$\delta r_{\text{cir}} = r_i \frac{\pi}{N} [e^{mN/(2\pi\Sigma_0)} + 1], \quad (10)$$

while  $\delta r_{\text{rad}}$  is the radial separation between ring  $i + 1$  and ring  $i$ ,

$$\delta r_{\text{rad}} = r_i [e^{mN/(2\pi\Sigma_0)} - 1]. \quad (11)$$

Therefore the mass of one particle is given by

$$m = \frac{2\pi\Sigma_0}{N} \log \left( \frac{N + \pi}{N - \pi} \right). \quad (12)$$

Note that we must set  $N > 3$ . In other words, we need at least four particles in each ring.

Now we consider the disc with  $\alpha \neq -2$ . The value of  $r_i$  is given by

$$2\pi\Sigma_0 \frac{r_i^{\alpha+2}}{|\alpha+2|} = mN \left( i - \frac{1}{2} \right). \quad (13)$$

Therefore the parameter  $\delta r_{\text{cir}}$  is

$$\delta r_{\text{cir}} = r_i \frac{\pi}{N} \left[ \left( \frac{i + \frac{1}{2}}{i - \frac{1}{2}} \right)^{1/(\alpha+2)} + 1 \right], \quad (14)$$

while  $\delta r_{\text{rad}}$  is

$$\delta r_{\text{rad}} = \left| r_i \left[ \left( \frac{i + \frac{1}{2}}{i - \frac{1}{2}} \right)^{1/(\alpha+2)} - 1 \right] \right|. \quad (15)$$

We can see that  $\epsilon$ , which is given by equation (9), depends on  $i$ . Thus the optimal  $m$  depends on  $i$  and the error cannot be zero for all  $i$ . Therefore we derive  $m$  which makes the largest error in a disc the smallest. Here, the derivative of  $\epsilon$  with respect to  $r_i$  is given by

$$\frac{d\epsilon}{dr_i} = \frac{di}{dr_i} \left( \frac{\pi}{N(\alpha+2)\delta r_{\text{cir}}} - \frac{1}{|\alpha+2|\delta r_{\text{rad}}} \right) \frac{-1}{(i - \frac{1}{2})^2}, \quad (16)$$

or

$$\frac{d\epsilon}{dr_i} = \frac{di}{dr_i} \left( \frac{\pi}{N(\alpha+2)\delta r_{\text{cir}}} + \frac{1}{|\alpha+2|\delta r_{\text{rad}}} \right) \frac{1}{(i + \frac{1}{2})^2}. \quad (17)$$

In addition, it is obvious that

$$\frac{di}{dr_i} > 0, \quad (18)$$

for all  $r_i$ . These equations indicate that  $\epsilon$  is a monotonic function of  $r_i$ . Therefore the largest absolute value of the error is either at  $r_{\text{in}}$  or  $r_{\text{out}}$  and  $N$  satisfies that the errors at  $r_{\text{in}}$  or  $r_{\text{out}}$  are same.

$$N = \pi \sqrt{\frac{[A(r_{\text{in}}) + 1][A(r_{\text{out}}) + 1]}{[A(r_{\text{in}}) - 1][A(r_{\text{out}}) - 1]}}, \quad (19)$$

where

$$A(r_i) = \left[ 1 + \frac{mN}{2\pi\Sigma_0} \frac{|\alpha+2|}{r_i^{\alpha+2}} \right]^{1/(\alpha+2)}, \quad (20)$$

by using equation (13). In this case we cannot set  $N$  arbitrarily. For example we set the initial point  $r_{\text{cut}}$  where we

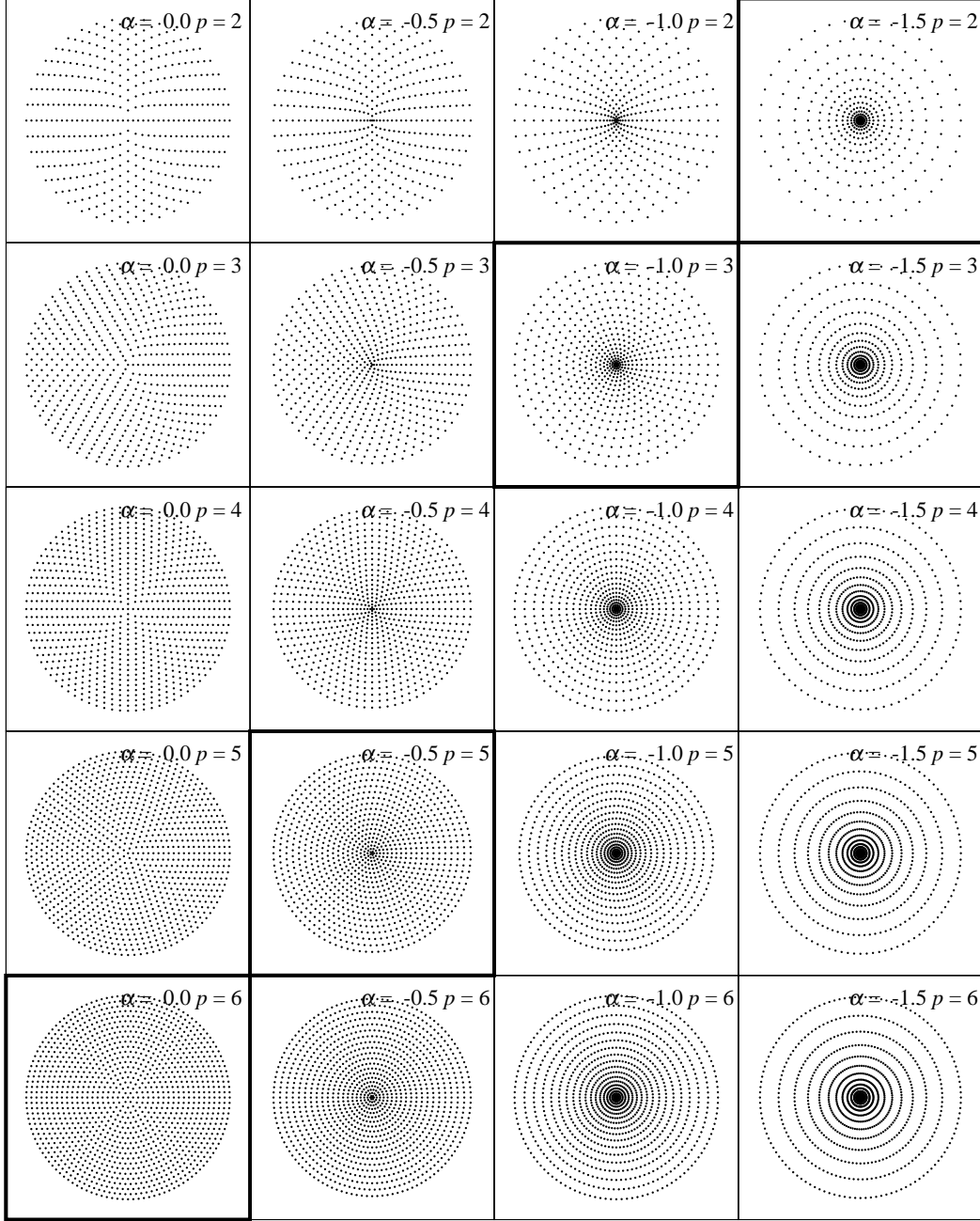


**Figure 3.** Examples of particle placements with  $p = 2 - 6$  and the density profile with  $\alpha = -1.5 - 0$ . The values of  $p$  are 2, 3, 4, 5, 6 from top to bottom and  $\alpha$  are 0,  $-0.5$ ,  $-1$ ,  $-1.5$  from left to right.

start to place particles and  $i_{\text{cut}}$  which is  $i$  at  $r_{\text{cut}}$ . Then  $r_{\text{cut}}$  and  $i_{\text{cut}}$  are give by

$$2\pi\Sigma_0 \frac{r_{\text{cut}}^{\alpha+2}}{|\alpha+2|} = mN \left( i_{\text{cut}} - \frac{1}{2} \right). \quad (21)$$

Therefore we can deform equation (20) as

$$A(r_i) = \left[ 1 + \frac{r_{\text{cut}}^{\alpha+2}}{r_i^{\alpha+2} (i_{\text{cut}} - \frac{1}{2})} \right]^{1/(\alpha+2)}. \quad (22)$$

By using equation (21),  $m$  is given by

$$m = \frac{2\pi\Sigma_0}{N (i_{\text{cut}} - \frac{1}{2})} \frac{r_{\text{cut}}^{\alpha+2}}{|\alpha+2|}. \quad (23)$$

In figure 5, the panel in the left-hand side shows an example of the particle placement with  $\alpha = -2$ , while the panel in the right-hand side shows that with  $\alpha = -1.9$ . We set  $r_{\text{in}} = 1$  and  $r_{\text{out}} = 5$ ,  $N = 40$  for  $\alpha = -2$ , and  $r_{\text{in}} = 1$  and  $r_{\text{out}} = 5$  for  $\alpha = -1.9$ . We can see that they actually

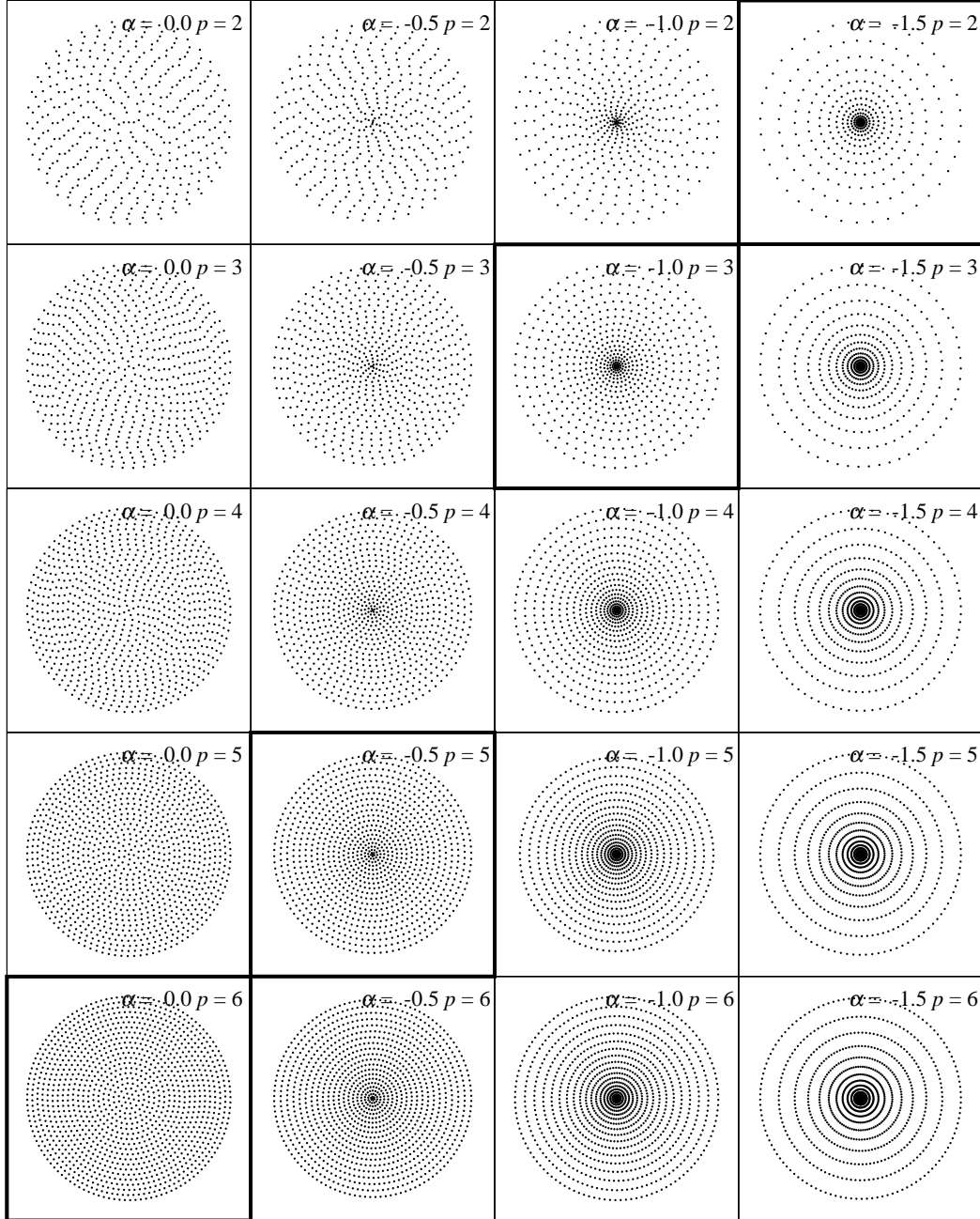


**Figure 4.** These are same with figure 3, but particles rotate randomly for every ring.

realize nearly equal radial and circumferential separations of particles.

#### 2.4 The optimization for small $p$

There are rounding error of  $p$  in equation (7). It is not so large, but not negligible in particular if  $p$  is small. In this section, we show that a simple offset can be used to reduce

this error. We introduce a constant term  $\beta$  into equation (4).

$$r_{\text{pow}} = \left[ \frac{(\alpha + 2)}{2} r_{\text{uni}}^2 + \beta \right]^{1/(\alpha+2)}. \quad (24)$$

The optimal  $p$  is now given by

$$p = \pi(\alpha + 2) \frac{r_i^{2+\alpha}}{r_i^{2+\alpha} - (\alpha + 2)\beta}. \quad (25)$$

Because  $p$  depends on  $r_i$ , we cannot get rid of the error at all  $r_i$ . Thus we introduce  $r_{\text{off}}$  where the rounding error is



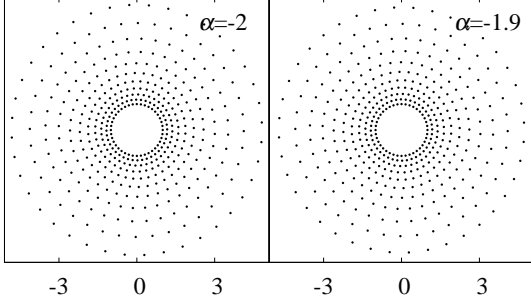


**Figure 5.** The left-hand side shows the example of particle placements with  $\alpha = -2$ , while the right-hand side shows that with  $\alpha = -1.9$ .

zero. Therefore the optimal  $\beta$  satisfies

$$\frac{r_{\text{off}}^{2+\alpha}}{r_{\text{off}}^{2+\alpha} - (\alpha + 2)\beta} = \frac{p_{\text{int}}}{p_{\text{real}}}, \quad (26)$$

where  $p_{\text{real}}$  equals to  $\pi(\alpha + 2)$  and  $p_{\text{int}}$  is given by the round-off value of  $p_{\text{real}}$ . Therefore  $\beta$  is given by

$$\beta = \gamma \frac{r_{\text{off}}^{\alpha+2}}{\alpha + 2}, \quad (27)$$

where

$$\gamma = 1 - \frac{p_{\text{real}}}{p_{\text{int}}}. \quad (28)$$

Here, we derive the optimal  $r_{\text{off}}$  which satisfies that the largest absolute value of the error in a disc is the smallest. From equation (25), we define the error  $\epsilon$  as

$$\epsilon = 1 - \frac{p_{\text{real}}}{p_{\text{int}}} \frac{r_i^{\alpha+2}}{r_i^{\alpha+2} - \gamma r_{\text{off}}^{\alpha+2}}. \quad (29)$$

The derivative of  $\epsilon$  with respect to  $r_i$  is given by

$$\frac{d\epsilon}{dr_i} = \frac{p_{\text{real}}}{p_{\text{int}}} \frac{(\alpha + 2)\gamma r_i^{\alpha+1} r_{\text{off}}^{\alpha+2}}{[r_i^{\alpha+2} - \gamma r_{\text{off}}^{\alpha+2}]^2}, \quad (30)$$

It shows that  $\epsilon$  is a monotonic function with respect to  $r_i$ . Therefore, as we derived in section 2.3, the errors at  $r_{\text{in}}$  and  $r_{\text{out}}$  is same when the largest error is the smallest. Therefore  $r_{\text{off}}$  satisfies

$$r_{\text{off}}^{\alpha+2} = \frac{(\gamma + 1)r_{\text{ave}}}{4\gamma} \left[ 1 - \sqrt{1 - \frac{16\gamma r_{\text{in}}^{\alpha+2} r_{\text{out}}^{\alpha+2}}{(\gamma + 1)^2 r_{\text{ave}}^2}} \right], \quad (31)$$

where  $r_{\text{ave}} = (r_{\text{in}}^{\alpha+2} + r_{\text{out}}^{\alpha+2})/2$ .

In figure 6, we show the sample particle placement for  $\alpha = -1.45$ . We set  $r_{\text{in}} = 1$  and  $r_{\text{out}} = 4$ . We also set  $r_{\text{cut}} = 1$  and  $i_{\text{cut}} = 20$ , where  $r_{\text{cut}}$  is the start point to place particles and  $i_{\text{cut}}$  is  $i$  at  $r_{\text{cut}}$ . The left-hand side shows the placement without the offset, while the right-hand side shows that with the offset. The difference is not so large. However, in figure 7, we can see that the error is smaller with the offset.

### 3 A GENERALIZED ALGORITHM FOR ARBITRARY DENSITY PROFILES

In section 2, we formulated algorithms to place particles on concentric rings, in order to realized discs of uniform den-

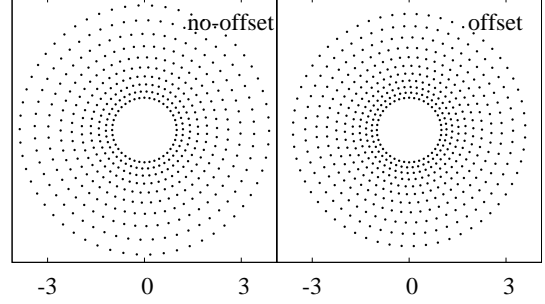


**Figure 6.** The left-hand side shows the example of particle placements without the offset, while the right-hand side shows that with the offset.

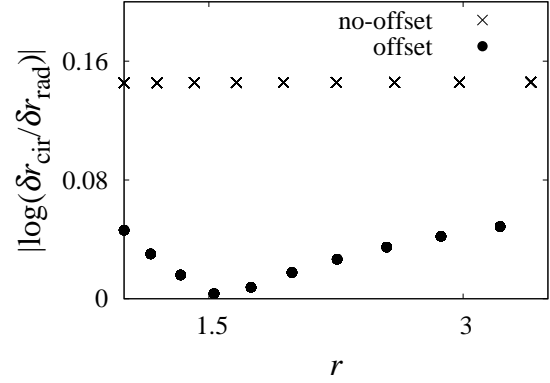


**Figure 7.** The difference between the radial and the circumferential separations of the placement without the offset and that with the offset.

sity and single power-law density profiles. In this section, we generalize the algorithms described in section 2 to general density distributions, in such a way that the generalized algorithm, when applied to the uniform profile, is reduced to the original algorithm.

In order to derive a generalization, we start from equation (7), and regard this equation as the formula to determine how many particles should be in the ring outside (or inside) the current one, from the *local* density slope.

We consider the case of a density profile given by  $\Sigma(r)$ . The local power-law index,  $\alpha(r)$ , is defined as

$$\alpha(r) = \frac{d \log \Sigma(r)}{d \log r} = \frac{d \Sigma(r)}{dr} \frac{r}{\Sigma(r)}. \quad (32)$$

At  $r_{\text{cut}}$  where we start to place particles, we assume that a single power-law disc with  $\alpha = \alpha(r_{\text{cut}})$  (hereafter  $\alpha_{\text{cut}}$ ) exists, and is expressed by  $i_{\text{cut}}$  rings of particles each with  $p_{\text{cut}} i$  particles, where  $p_{\text{cut}}$  is chosen to satisfy equation (7) for  $\alpha = \alpha_{\text{cut}}$ .

Now we can determine the mass and the number of particles to be placed at  $r_{\text{cut}}$ , by following the scheme we presented in section 2.4. Since we want to minimize the error given by equation (29) at  $r_{\text{cut}}$ , we set  $r_{\text{off}}$  to be equal to

$r_{\text{cut}}$ . We now need to determine  $r_{\text{cut}}$  which minimizes the error defined in equation (9). In principle, we can follow the derivation we used in section 2.4, and perform non-linear optimization to obtain the optimal value of  $r_{\text{cut}}$ . In practice, it would be sufficient to set  $r_{\text{cut}}$  equal to  $r_{\text{in}}$ , since, as shown in figure 7, the optimal  $r_{\text{cut}}$  is much closer to  $r_{\text{in}}$  than to  $r_{\text{out}}$ . Note that in general the error diverges in the limit of  $r \rightarrow 0$ , but stays finite in the limit of  $r \rightarrow \infty$  (in the case of  $\alpha > -2$ ).

The total mass of the assumed disc inside  $r_{\text{cut}}$  is given by

$$M(r_{\text{cut}}) = \frac{2\pi\Sigma(r_{\text{cut}})r_{\text{cut}}^2}{(\alpha_{\text{cut}} + 2)} \frac{p_{\text{real}}(r_{\text{cut}})}{p_{\text{int}}(r_{\text{cut}})}, \quad (33)$$

and the number of particles in this region is  $i_{\text{cut}}^2 p_{\text{cut}}/2$ . Thus,

$$m = \frac{4\pi\Sigma(r_{\text{cut}})r_{\text{cut}}^2}{(\alpha_{\text{cut}} + 2)p_{\text{cut}}i_{\text{cut}}^2} \frac{p_{\text{real}}(r_{\text{cut}})}{p_{\text{int}}(r_{\text{cut}})}. \quad (34)$$

Note that this equation is valid for  $p \neq 0$ . The value of  $m$  for  $p = 0$  is given as section 2.3.

For the ring  $i+1$ , we place  $N_{i+1}$  particles at radius  $r_{i+1}$ , where  $N_{i+1}$  is given by

$$N_{i+1} = N_i + \frac{p_{i+1} + p_i}{2}. \quad (35)$$

Here,  $p_i$  is chosen to satisfy equation (7) for  $\alpha = \alpha(r_i)$ . The radius  $r_{i+1}$  where the next ring is placed, is given by

$$M(r_{i+1}) - M(r_i) = m(N_{i,\text{out}} + N_{i+1,\text{in}}). \quad (36)$$

Here,  $N_{i+1,\text{in}}$  is the number of particles at  $r_{i+1}$  and inside, while  $N_{i,\text{out}}$  is that at  $r_i$  and outside. The panel in the left-hand side of figure 8 shows the example of the particles in a ring. In the following we derive  $N_{i,\text{in}}$  and  $N_{i,\text{out}}$ .  $N_{i,\text{in}}$  is given by

$$N_{i,\text{in}} = \frac{p_i i - p_i}{2} + \zeta_i p_i. \quad (37)$$

Here, the first term is the number of particles on the sides of the  $p_i$ -gon, while the second term is that on vertices. The parameter  $\zeta_i$  is the fraction of particles on vertices in the inner annulus. It is given by

$$\zeta_i = \frac{(p_i - 2)}{2p_i}. \quad (38)$$

We illustrate an example of  $\zeta_i$  on the right-hand side panel of figure 8. Using equation (38), we have

$$N_{i,\text{in}} = \frac{p_i i - 2}{2}. \quad (39)$$

The value of  $N_i$  is  $p_i i$ , thus

$$N_{i,\text{in}} = \frac{N_i - 2}{2}. \quad (40)$$

The parameter  $N_{i,\text{out}}$  in equation (36) is given by

$$\begin{aligned} N_{i,\text{out}} &= \frac{p_i i - p_i}{2} + (1 - \zeta_i)p_i, \\ &= \frac{p_i i + 2}{2}. \end{aligned} \quad (41)$$

The value of  $N_i$  is  $p_i i$ , thus

$$N_{i,\text{out}} = \frac{N_i + 2}{2}. \quad (42)$$

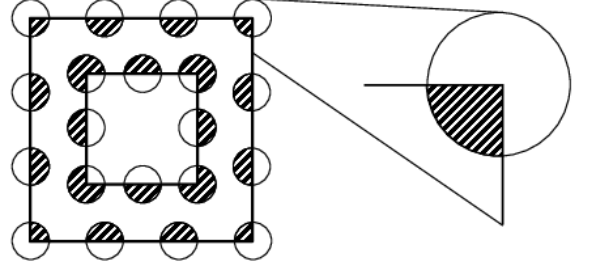


**Figure 8.** Particles with slanted lines in the left-hand side shows particles in an annulus in  $r = [r_2 : r_3]$  with  $p = 4$ . The right-hand side express  $\zeta_i$  in equation (38) with this annulus.

Therefore the total number of particles in the region between  $r_i$  and  $r_{i+1}$  is given by

$$N_{i,\text{out}} + N_{i+1,\text{in}} = \frac{N_i + N_{i+1}}{2}. \quad (43)$$

Therefore equation (36) becomes

$$M(r_{i+1}) - M(r_i) = m \frac{N_i + N_{i+1}}{2}. \quad (44)$$

One might think that the same result can be obtained in much simpler way, if one assume that half of one ring of particles belong to the outside annulus and the remaining half inside. This is true except for the innermost "annulus" or disc. In our interpretation, if we place one particle of the centre, this central particle fully belongs to the "outside" annulus, which is the innermost disc. In the simpler view, only the half of the mass can belong to the disc, and the remaining half belongs to nowhere.

By using equations (35) and (44), we can determine parameters of ring  $i+1$  implicitly.

We show two examples below. First, one is the exponential disc given by

$$\Sigma(r) = e^{-r}. \quad (45)$$

We set  $r_{\text{in}} = 1$ ,  $r_{\text{out}} = 4$  and  $i_{\text{cut}} = 15$ . The result is shown in the left-hand side of figure 9. We can see that the radial and the circumferential separations of particles are well balanced in the entire region. As the second example, we model the density profile of post-impact disc in Nakajima & Stevenson (2014).

$$\Sigma(r) = (C_1 + C_2 r)e^{-C_3 r}, \quad (46)$$

where  $C_1, C_2$  and  $C_3$  are constants. For stable post-impact discs, the gradient of the density is zero at the inner edge of the disc. We set  $C_1 = -1, C_2 = 1$  and  $C_3 = 1$ . Therefore  $r_{\text{in}} = 2$ . In addition we set  $r_{\text{out}} = 4$  and  $i_{\text{cut}} = 10$ . The result is shown in the right-hand side of figure 9. It shows that the radial and the circumferential separations of particles are also well balanced in the entire region.

## 4 DISCUSSION AND SUMMARY

### 4.1 Related works

As already mentioned in the introduction, C09 is probably the first to provide a general algorithm to place equal-mass particles on concentric rings to express an arbitrary

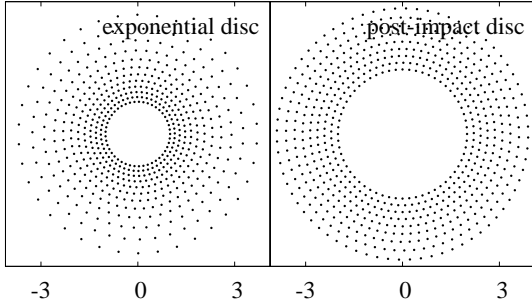


**Figure 9.** The left-hand side show particle placements with equation (45), while the right-hand side show that with equation (46).

radial density profile. Their “Quantized spiral placement” technique is, however, rather complicated, and even for a uniform disc, their technique require the entire procedure to be followed with care.

On the other hand, our algorithm is quite simple, in particular for discs of uniform density or single power-law density. Since what we need for the set-up of test calculation is these simple profiles, we believe our algorithm is of practical value. Also, even for general density profiles, our algorithm, in which we place rings one by one, is simple to implement and test.

For the case of the uniform disc, our algorithm is closely related to the area-conserving mapping between polygons and circles (See e.g. Shirley, P. & K. Chiu 1997). In fact, the mapping between square and circle in Shirley, P. & K. Chiu (1997) gives our algorithm with  $p = 8$  but with slightly modified radial locations (ring  $i$  at radius  $\Delta r(i + 0.5)$ ). Note that we need to use  $p = 6$  for the uniform disc to achieve the optimal ratio between the radial and the circumferential spacings, and other values for power-law discs. They can be regarded as mapping between  $p$ -gons and circles.

#### 4.2 An alternative algorithm for general discs

In section 3 we constructed an algorithm to place particles to reduce general discs, starting from equation (7). It is also possible to start from equation (9), which defines the local error. In this case, instead of using equation (35),  $r_{i+1}$  and  $N_{i+1}$  are determined so that the error given by equation (9) is minimized. We decided against using this procedure, because of the following reason. When we apply this alternative procedure for general disc, to simple power-law discs,  $\Delta N_i = N_{i+1} - N_i$  would show an oscillatory, to reduce the error shown in figure 7. This might not be a serious problem. However, for SPH calculation, this oscillation implies radial density perturbation which should not exist. Therefore we believe the alternative we described here has some unwanted characteristics.

#### 4.3 Summary

In this paper, we present a very simple algorithm to place equal-mass particles on concentric circles to express discs

of arbitrary density profiles. Our algorithm is much simpler than previously known one C09, and extremely simple for the case of uniform or power-law density profiles.

#### ACKNOWLEDGEMENTS

This work was supported by RIKEN Junior Research Associate Program and MEXT SPIRE and JICFuS.

#### REFERENCES

- Balsara, D. S. 1995, *Journal of Computational Physics*, 121, 357
- Cartwright, A., Stamatellos, D., & Whitworth, A. P. 2009, *MNRAS*, 395, 2373
- Cullen, L., & Dehnen, W. 2010, *MNRAS*, 408, 669
- Hopkins, P. F. 2015, *MNRAS*, 450, 53
- Imaeda, Y., & Inutsuka, S.-i. 2002, *ApJ*, 569, 501
- Morris, J. P., & Monaghan, J. J. 1997, *Journal of Computational Physics*, 136, 41
- Nakajima, M., & Stevenson, D. J. 2014, *Icarus*, 233, 259
- Shirley, P., & K. Chiu, 1997, *JGT*, 2(3), 45-52

This paper has been typeset from a  $\text{\LaTeX}$  file prepared by the author.